



HAL
open science

Impact of fluidized bed granulation on structure and functional properties of the agglomerates based on the durum wheat semolina

Bettina Bellocq, Bernard Cuq, Thierry Ruiz, Agnès Duri-Bechemilh, Kevin Cronin, Denis Ring

► To cite this version:

Bettina Bellocq, Bernard Cuq, Thierry Ruiz, Agnès Duri-Bechemilh, Kevin Cronin, et al.. Impact of fluidized bed granulation on structure and functional properties of the agglomerates based on the durum wheat semolina. *Innovative Food Science & Emerging Technologies / Innovative Food Science and Emerging Technologies* , 2017, 45, 10.1016/j.ifset.2017.09.001 . hal-01606829

HAL Id: hal-01606829

<https://hal.science/hal-01606829>

Submitted on 26 May 2020

HAL is a multi-disciplinary open access archive for the deposit and dissemination of scientific research documents, whether they are published or not. The documents may come from teaching and research institutions in France or abroad, or from public or private research centers.

L'archive ouverte pluridisciplinaire **HAL**, est destinée au dépôt et à la diffusion de documents scientifiques de niveau recherche, publiés ou non, émanant des établissements d'enseignement et de recherche français ou étrangers, des laboratoires publics ou privés.



Distributed under a Creative Commons Attribution - ShareAlike 4.0 International License

1 **Impact of fluidized bed granulation on structure and functional properties of the**
2 **agglomerates based on the durum wheat semolina**

3
4 Bettina Bellocq¹, Bernard Cuq¹, Thierry Ruiz¹, Agnès Duri¹, Kevin Cronin², Denis Ring²

5
6 ¹UMR IATE 1208 CIRAD/INRA/Montpellier SupAgro/Université Montpellier.

7
8 ²Department of Process & Chemical Engineering, University College, Cork, Ireland.

9
10
11 **Abstract** - The granulation step determines the production yield and the final characteristics
12 of the agglomerated couscous grains of durum wheat. The objective of the present work was
13 to explore the capability of the fluidised bed technology to produce agglomerates of durum
14 wheat semolina. The impacts of different processing conditions have been investigated on the
15 structure and functional properties of the agglomerates. The size, shape, water content,
16 compactness, and mechanical strength of the granules were measured. The fluidized bed
17 agglomeration process has been found to produce agglomerates of durum wheat with
18 different attributes compared to those produced by granulation using the low shear mixers.
19 The results were discussed in regard to the hydro-textural approach, in order to get a better
20 understanding of the mechanisms and relationships between process, structure, and
21 properties. Two major agglomeration mechanisms contribute to the growth of the wet
22 agglomerates: a fractal-structuring process followed by a phenomenon of densification. By
23 studying the evolution of the compactness, diameter and water content, it was demonstrated
24 that inter granular arrangements led to an expansion followed by a densification of the wet
25 agglomerates. A relationship was proposed to describe the growth using a fluidized bed of the
26 wet agglomerates of durum wheat semolina.

27
28 **Keywords** - Fluidized bed ; agglomeration ; couscous grains structure ; hydrotextral
29 diagramm

31 1. Introduction

32 Wet agglomeration is based on the coupling of two phenomena: mixing the powder and
33 incorporating a binder. The structuration of associated sticky particles takes place under shear
34 stress (Iveson, Litster, Hapgood, & Ennis, 2001). Agglomeration of powders using a fluidized
35 bed has been largely investigated either in batch or in open mode (Boerefijn & Hounslow,
36 2005; Nienow, 1995; Philippsen, Vilela, & Zen, 2015; Rambali, Baert, & Massart, 2001;
37 Rieck, Hoffmann, Bück, Peglow, & Tsotsas, 2015; Turchiuli et al., 2005; Zhai et al., 2009).
38 This technology can be used to agglomerate powders by spraying a binder solution directly
39 onto the fluidised powder bed (Saleh & Guigon, 2009; Turchiuli, Eloualia, El Mansouri, &
40 Dumoulin, 2005). The growth mechanisms of the agglomerates depend on the ability of
41 process parameters to activate the surface reactivity of particles and promote collisions. The
42 liquid binder is usually distributed by means of an atomising nozzle, above or inside the
43 powder bed. A vertical air stream agitates the fluidized particle's bed and contributes to the
44 heat and moisture transfers. Several simultaneous and/or competitive mechanisms occur
45 (wetting/drying, growth/rupture, swelling/shrinkage, consolidation, chemical reactions...)
46 and contribute to the agglomeration (Leuenberger, Puchkov, Krausbauer, & Betz, 2009).
47 Spray nozzle orientation and design, binder flow rate, flows and distribution of the
48 fluidization gas inside the processing chamber, relative humidity, and temperature are the
49 multiple process parameters involved (Jacob, 2007; Pathare, Baş, Fitzpatrick, Cronin, &
50 Byrne, 2012). As the binding liquid is sprayed as small droplets, the agglomeration
51 mechanisms are initiated by the coating of the native particles. The formation of initial nuclei
52 is followed by the coalescence mechanisms (Banjac, Stakic, & Voronjec, 1998; Barkouti,
53 Turchiuli, Carcel, & Dumoulin, 2013; Turchiuli, Smail, & Dumoulin, 2013). The pneumatic
54 agitation of the powder bed produces collisions between the wetted particles that could
55 coalesce by the formation and the persistence of liquid bridges. The growth of granules is
56 also affected by the rupture mechanisms of the structures due to shear stress between the wall
57 and/or breakage induced by the intensity of the collisions. The distinction between these
58 coupled phenomena in terms of rate and spatial localisation in the reactor represents a
59 challenge to improve agglomeration (Hemati, Cherif, Saleh, & Pont, 2003; Smith & Nienow,
60 1983). The shape and texture of the agglomerates are essentially depending on the
61 mechanical environment generated in the reactor. Due to the low shear stresses developed by
62 the air flow, the granules formed using a fluidised bed are generally more porous and have

63 more irregular shape than those produced by using rotating drums and mechanical shear
64 mixer (Jacob, 2007; Ji, Fitzpatrick, Cronin, Fenelon, & Miao, 2017; Morin & Briens, 2014).

65 The food powders can be agglomerated to improve their properties (e.g. size distribution,
66 shape, flowability, instant properties, colour, *etc.*) (Barkouti et al., 2013; Dacanal &
67 Menegalli, 2010; Palzer, 2011). Fluid bed agglomeration has been used to improve the instant
68 properties and the flowability of dairy powders, instant coffee, cocoa beverages, or culinary
69 powders (Palzer, 2011; Turchiuli et al., 2013). The binder solution is simply water when
70 processing amorphous water-soluble particles, but viscous liquids are used to agglomerate
71 crystalline water-soluble particles (Cuq, Mandato, Jeantet, Saleh, & Ruiz, 2013). The
72 agglomeration is a key operation in the elaboration of couscous grains of durum wheat
73 semolina (Barkouti, Rondet, Delalonde, & Ruiz, 2012; Saad, Barkouti, Rondet, Ruiz, & Cuq,
74 2011). Industrial couscous grains are made by successive operations: wet agglomeration,
75 rolling, cooking, drying, and screening. In the industrial context, the durum wheat semolina is
76 granulated using mechanical low shear mixers, to imitate the traditional homemade
77 processing (Abecassis, Cuq, Boggini, & Namoune, 2012). Wet granulation stage is one of the
78 critical stage that determines the production yield, the final size, shape and functionalities of
79 the couscous grains (Barkouti, Delalonde, Rondet, & Ruiz, 2014; Hafsa et al., 2015; Hébrard,
80 2002; Oulahna, Hebrard, Cuq, Abecassis, & Fages, 2012; Saad et al., 2011). Only few
81 technical and scientific works are available to rationalize the management of the process,
82 which restricts the potential of rupture innovation by only optimization and incremental
83 solutions.

84 The objective of the present paper is to explore the capability of the fluidised bed technology
85 to produce agglomerates of durum wheat semolina. The impact of different processing
86 conditions on the structure characteristics and functional properties of the agglomerates have
87 been investigated by experiments. Results are discussed in regard to the hydrotextral
88 approach (Thierry Ruiz, Rondet, Delalonde, & Desfours, 2011), in order to get a better
89 representation and understanding of the mechanisms and relationships between process,
90 structure, and properties.

91

92 2. Material and Methods

93

94 2.1. Raw materials

95 Two different durum wheat semolina were used as raw material for the agglomeration
96 experiments: standard industrial semolina (Panzani group, France) and coarse semolina
97 (UMR IATE, France). Semolina were stored in hermetic containers at 4°C until experiments
98 were carried out. Semolina were characterized using standardized methods (Table 1). The
99 water content was determined according to the approved method 44-15A (AACC, 2000), by
100 weighing after oven drying at 105°C for 24 h. The characteristics values of particle diameters
101 were measured by a laser particle size analyser (Coulter TMLS 230, Malvern, England) at
102 room temperature. The semolina true dry density (ρ_s^*) was measured by using a nitrogen
103 pycnometer (ULTRAPYC 1200e, Quatachrom) after oven drying at 105°C for 24 h. The
104 semolina apparent density (ρ) was measured by a hydrostatic balance (RB 360, WC Heraeus
105 GmbH, Hanau, Germany). From these values, the compactness of the semolina particles at
106 each water content was calculated as: $\phi_P = \frac{\rho}{(1+w) \cdot \rho_s^*}$. The total nitrogen content (TN) of
107 semolina was determined by the Kjeldahl method, and the crude protein content was
108 calculated according to TN-5.7 based on the AFNOR method V 03-050 (AFNOR, 1970). All
109 experimental measurements were carried out in triplicate.

110

111

112 2.2. Agglomeration process

113 The wet agglomeration process was conducted by using a glass fluidised bed granulator
114 (Mini-Airpro, Procept, Belgium) (Fig. 1), whereby the lower portion is conical in shape and
115 the upper portion is cylindrical (height = 0.73 m). Water was used as the liquid binder. Water
116 was sprayed using a nozzle in a downward direction (*i.e.* in the counter current to the air
117 flow). The temperature of the inlet airflow was kept constant during experiments (25°C) and
118 controlled using a temperature probe (Fig. 1). A constant weight of semolina (300 g) was first
119 introduced inside the unit and was fluidized by ascendant airflow at constant rate (0.70
120 m³/min) for 2 min to equilibrate the temperature. The flow rate of water was kept constant
121 using a peristaltic pump (8 mL/min), and controlled by the continuous measurement of the
122 weight of the water tank. The time for water addition (3, 6, 9, 12.5, or 16.3 min) was defined
123 in regards with the amount of added water (24, 48, 72, 100, or 130 g) that was incorporated
124 inside the reactor, in order to reach specific amount of added water (0.08, 0.16, 0.24, 0.33, or

125 0.43 g of added water / g of semolina), and specific values of apparent process water contents
126 (0.24, 0.33, 0.42, 0.53, or 0.65 g of water / g dry matter). Due to the simultaneous drying
127 mechanisms occurring during processing, the values of the apparent process water content
128 were significantly higher than the true water content measured in the bed at the end of the
129 process (Fig. 2). An almost constant value of the drying rate (11.0 ± 0.9 g of water / min) was
130 determined whatever the process conditions. Immediately after the end of the water addition
131 stage, the wet agglomerates were collected. Trials were conducted in triplicate.

132

133

134 2.3. Cooking and drying process

135 Immediately after the agglomeration stage, the collected wet agglomerates were sieved over a
136 column of 2 metallic sieves of decreasing mesh (1.4 and 0.85 mm) for 2 min at ambient
137 temperature. The sieve column was softly shaken manually to limit the possible breakage of
138 the wet agglomerates. The range of mesh size was determined in regards with the capacities
139 of the experimental equipment and with the values classically used for the industrial
140 production of the couscous grains. The wet agglomerates that were collected over the 0.85
141 mm sieve, were immediately spread as a thin layer (about 3 mm) over a stainless steel plate
142 inside a steam cooker (Kenwood rice cooker RC310), and steamed for 10 min at 100°C using
143 saturated steam at atmospheric pressure. The steamed agglomerates were immediately
144 collected, spread as a thin layer (about 3 mm) over stainless steel mesh and then drying in an
145 oven (GallenKamp Plus II oven 150L) for 25 min at 50°C and 15% relative humidity. The
146 dried agglomerates were collected and stored inside hermetic plastic cups until
147 characterization.

148

149

150 2.4. Characterization of the agglomerates

151 Water content - The water content (w) of agglomerates (dry base) was determined on 3-5 g
152 samples, by a drying method in an oven at 105°C for 24 h (AACC, Method 44-15A): $w =$
153 m_w/m_s , m_w is the mass of water (g) and m_s is the mass of dry matter (g) in the sample. Mean
154 values were determined from triplicate.

155

156 Compactness - The compactness of the agglomerates (ϕ) is calculated using Eq. (1).

157

$$\phi = \frac{V_s}{V} = \frac{m_s}{V \cdot \rho_s^*} \quad (1)$$

159

160 Where V_s is the solid volume of the agglomerate (cm^3 of solid matter); V is the total volume
 161 of the agglomerate (cm^3); m_s is the solid mass (g of dry matter), ρ_s^* is the solid real density of
 162 durum wheat semolina. The apparent volume (V_a) of the agglomerates was measured by
 163 using a Camsizer (Retsch, Germany) digital image analyser. The solid mass (m_s) was
 164 measured with a digital balance with sensitivity of 0.001 g. In the case of unsaturated
 165 structures, the compactness is a function of the water content and the saturation degree
 166 ($S=V_w/V_{\text{void}}$) and for strictly wet media ($0 < S \leq 1$) Eq. (2) can be written as follow:

167

$$\phi(w, S) = \frac{1}{1+d_s^*w/S} \quad (2)$$

169

170 Size distribution of the wet agglomerates - The wet agglomeration process generates
 171 agglomerates with dispersed sizes, which were measured directly after the agglomeration
 172 stage. Size distribution was determined by sieving all the collected agglomerates over a
 173 column of 7 metallic sieves of decreasing mesh size (3.35, 2.8, 2.36, 1.40, 0.85, 0.71, and
 174 0.425 mm). The sieve column was manually shaken for only 1 min, to limit the possible
 175 particle breakage. The size distribution was obtained by weighing the mass of agglomerates
 176 remaining on each sieve. The weight distribution according to size criteria was expressed as
 177 the percent of total weight. Even if the particle size distribution curves were not fully
 178 unimodal, the apparent median diameter (d_{50}) and apparent span: $(d_{90}-d_{10})/d_{50}$, of the size
 179 distribution were calculated as global apparent descriptors. The agglomerates, that were
 180 collected on the sieves of 0.425, 0.71, 0.85, 1.40, or 2.36 mm mesh size, were characterized
 181 by their size, water content, and compactness.

182

183 Median diameter of the dried agglomerates - Samples of agglomerates (about 10 g) were
 184 used to determine the median diameter on each sieve, using the Camsizer (Retsch, Germany)
 185 digital image analyser. Particle size distributions were characterized by the value of the
 186 median diameter. Measurements were conducted in triplicate.

187

188 Agglomerates shape – The sphericity of the dried agglomerates was determined by using the
 189 Camsizer (Retsch, Germany) digital image analyser. Samples of agglomerates (about 10 g)
 190 were used. Sphericity is a aspect ratio defined by the measurement of the length/width

191 relationship. The values range between 0 (perfect circle) and 1 (needle shaped object).
192 Measurements were conducted in triplicate.

193

194 Agglomerates microstructure - The microstructure of the dried agglomerates was observed by
195 scanning electron microscopy (Inspect F by FEI operating at 5kV). A sample of agglomerates
196 was dispersed on a conducting carbon tape prior to analysis. Representative pictures were
197 selected for each sample.

198

199 Agglomerates strength - The strength of the dried agglomerates was measured using a texture
200 analyser (TA-HD Plus, Stable Micro Systems, UK). The agglomerates strength is defined as
201 the force needed to compress one agglomerate over a distance of 400 μm . A 5 kg load cell
202 was used with a compressive probe operating at 100 $\mu\text{m}\cdot\text{s}^{-1}$. Texture experiments were
203 conducted by characterizing the agglomerates one by one. It was thus not possible to
204 characterize a large number of agglomerates. A restricted number of agglomerates (about 10)
205 having some homogeneity in their size, to be statistically representative of the sample were
206 tested. Mean values were determined from 10 measurements.

207

208 *2.5. Statistical analysis*

209 The statistical significance of results was assessed using single factor analysis of variance
210 (ANOVA). Multiple comparisons were performed by calculating the least significant
211 difference using Microsoft Excel 2010, at a 5% significance level.

212

213

214 3. Results

215

216 3.1. Characterisation of the wet agglomerates after the agglomeration stage

217 The wet agglomeration process by using the fluidized bed was first conducted with the
218 standard semolina and apparent process water content of 0.53 g/g dry matter. As expected,
219 the wet agglomerates collected after the fluidized bed processing were characterized by high
220 values of measured water content (0.37 ± 0.04 g/g dry matter) and low values of compactness
221 (0.41 ± 0.04), compared to the native semolina particles (0.148 g/g dry matter and 0.85,
222 respectively). The size distribution of the wet agglomerates (Fig. 3) demonstrated a relatively
223 large range in the diameter values (from 500 to more than 4000 μm), with median diameter
224 (d_{50}) close to 650 μm (± 3 μm). The value of the span (2.27) was relatively low, indicating
225 that the majority of the grains were centred on the median diameter. The mass fraction of the
226 wet agglomerates with diameter ranging between 1000 and 2000 μm was about 40%. This
227 value is almost similar than the mass yield usually observed during the industrial processing
228 of the couscous grains using low shear mechanical mixers (Abecassis et al., 2012).

229 The physicochemical characteristics of the wet agglomerates were measured for each class of
230 agglomerates as a function to their diameter (Fig. 4). The water content of the wet
231 agglomerates was positively correlated with their diameter (Fig. 4a). Similar positive
232 correlations have already been observed for the wet agglomerates of durum wheat semolina
233 processed by the mechanical mixing under low shear conditions (Barkouti et al., 2012;
234 Bellocq, Ruiz, Delaplace, Duri, & Cuq, 2017).

235 The increase in the median diameter of the wet agglomerates is also associated to changes in
236 compactness (Fig. 4b). The compactness of the wet agglomerates decreases (from 0.43 to
237 0.36) with an increase in the median diameter until 1600 μm . Above 1600 μm , the
238 compactness tends to increase as the median diameter increases.

239 The results also demonstrated a positive relationship between the values of sphericity and the
240 diameter of the wet agglomerates (Fig. 4c). The large agglomerates were more spherical than
241 the small ones. It should be noticed that the wet agglomerates with diameters between 1000
242 and 2000 μm were characterized by high values of sphericity (0.82 - 0.87) and low values of
243 compactness (0.36 - 0.40), when compared to the wet agglomerates obtained by using a low
244 shear mechanical mixer (0.67 and 0.61, respectively) (Bellocq et al., 2017).

245

246

247 3.2. Impact of the process parameters of the fluidized bed

248

249 3.2.1. Impact of the amount of water

250 The impact of the water content of the bed was studied by applying different processing times
251 for water spraying. The physicochemical characteristics of the wet agglomerates were
252 measured for each class of wet agglomerates according to their diameter, and plotted for the
253 different measured true water content from 0.19 to 0.48 g/g dry matter (Fig. 5-7). Increasing
254 the water content did not significantly change the shape of the curve of the size distribution,
255 but generated higher amounts of the fractions of the large agglomerates (Fig. 5). An increase
256 in the water content improved the capability of the fluidised bed to produce higher amounts
257 of the wet agglomerates of larger diameter. The mass fraction of agglomerates between 1000
258 and 2000 μm reached a value of 66% when processed at 0.48 g / g dry matter.

259 An increase in the water content induced an almost linear increase in the median values (d_{50}
260 from 349 μm to 1032 μm) of the diameter (Fig. 6). The values of the diameter span were
261 constant (from 1.49 to 1.10) with true water content from 0.24 to 0.42 g/g dry matter. It then
262 increased with values of water content higher than 0.37 g/g dry matter.

263 The relationships between the diameter and measured water contents for the different wet
264 agglomerates did not change (Fig. 7a), whatever the amount of added water. There were
265 positive relationships between diameter and water content of the wet agglomerates. The large
266 agglomerates were more hydrated than the small ones.

267 The impact of an increase of the amount of added water on the measured water content of the
268 wet agglomerates depended on their diameter (Fig. 7a). Increasing the amount of water
269 largely increased the water content of the agglomerates. We could suppose that the fluidized
270 bed homogeneously distributed the added water over the small grains and the grains of
271 intermediate size.

272 An increase in the amount of added water decreased the compactness of the wet
273 agglomerates, irrespectively of their diameter. Nevertheless, increasing the amount of added
274 water did not significantly change the dependence observed previously, between the
275 compactness and the diameter of the wet agglomerates (Fig. 7b). The compactness decreased
276 with an increase in the median diameter until a median diameter close to 1600 μm . The
277 compactness then slightly increase with an increase in diameter above 1600 μm . Similar
278 phenomena were observed whatever the amount of added water added during processing.

279 Whatever the amount of added water, the large agglomerates were more spherical than the
280 small ones (Fig. 7c). An increase in the amount of water did not have a significantly impact

281 on the sphericity of the wet agglomerates. The wet agglomerates were characterized by the
282 same values of sphericity, depending on their diameter.

283

284

285 *3.2.2. Impact of the particle size of the native semolina*

286 We evaluated the influence of the diameter of the native raw material, by comparing the
287 agglomeration behaviour of the standard semolina ($d_{50} = 280 \mu\text{m}$) and coarse semolina ($d_{50} =$
288 $619 \mu\text{m}$) (Fig 8-9). It was possible to produce wet agglomerates by the fluidised bed using the
289 coarse semolina. Using coarse semolina favoured the production of larger wet agglomerates
290 (Fig 8), with higher value of median diameter ($d_{50} = 1273 \mu\text{m}$) and similar span (2.11), when
291 compared to those previously determined using the standard semolina ($d_{50} = 650 \mu\text{m}$ and
292 span = 2.27). It is recognized that the wet agglomeration process increases the diameter of the
293 structures of approximately a decade, regarding to the size of the native particles (T. Ruiz,
294 2012).

295 Using the coarse semolina gave wet agglomerates with lower values of water content and
296 compactness (Fig 9a-9b). By incorporating the same amount of water in the fluidized bed
297 (100 g), we could expect the same measured water content in the bed and for the wet
298 agglomerates at the end of the wet agglomeration, whatever the type of semolina. However,
299 the measured water content of the collected powder is close to $0.30 \pm 0.04 \text{ g/g dry matter}$,
300 which is broadly lower than the value measured using the standard semolina ($0.37 \pm 0.04 \text{ g/g}$
301 dry matter). The lower values of compactness of the wet agglomerated of coarse semolina
302 could lead to higher water evaporation mechanisms during fluidized bed processing and to
303 lower values of water content.

304 Using the coarse semolina significantly affected the values of sphericity (Fig 9c). A slight
305 decrease in the values of sphericity was observed from the small to the large wet
306 agglomerates, while a positive relationship was demonstrated for the standard semolina. The
307 large agglomerates were less spherical than the small ones. It could be more difficult to form
308 a spherical grain with fewer and larger particles.

309

310

311 *3.3. Characterisation of the agglomerates after cooking and drying*

312 After sieving, the wet agglomerates that were collected between the sieves 850 and 1400 μm
313 were processed by two successive stages: steam cooking and final drying. The

314 characterization of the agglomerates was conducted after the cooking stages and after the
315 final drying stage (Fig. 10 and Table 2).

316 The steam cooking stage and the drying stage did not change the shape of the distribution
317 curves of the diameters of the agglomerates of semolina (Fig. 10). The size distribution of the
318 wet agglomerates was almost fixed by the wet granulation stage (Table 2) and only slightly
319 affected by the steam cooking stage and by the drying stage. The median diameter of the wet
320 agglomerates ($d_{50} = 910 \mu\text{m}$) was slightly increased by the subsequent steam-cooking stage
321 ($d_{50} = 1000 \mu\text{m}$) due to partial water absorption and swelling mechanisms. The final drying
322 stage slightly reduced the median diameter of the agglomerates through possible shrinking
323 mechanisms ($d_{50} = 950 \mu\text{m}$). The results also demonstrated that the span of the distribution of
324 the diameters of the wet agglomerates (0.47) was slightly increased by the cooking stage
325 (0.53) and by the drying stage (0.64). It could be associated with some breakage or collapse
326 mechanisms generated by these two stages, that increase the range of the diameters. The
327 present results indicated that distribution of the diameters of the agglomerates of durum
328 wheat was mainly controlled by the agglomeration process stage. This stage greatly
329 controlled the total yield of dried agglomerates production of correct diameter, according to
330 the classic couscous manufacturing.

331 The steam-cooking stage induces swelling caused by hydration. This phenomenon reduced
332 the compactness (0.30), which corresponds to the increase of the agglomerates volume
333 exactly due to the increasing of the water content (0.45 g/g dry matter) (Table 2). The
334 cooking stage promotes mechanisms of expansion due to water absorption and swelling
335 mechanisms, which take place at the scale of the wheat components. These heat and mass
336 transfers impact some physico-chemical changes under high temperature, such as starch
337 gelatinization. The swelling of the agglomerates seemed to be more important than the
338 progressive filling of their internal pore by the water molecules.

339 The drying stage induced an increase in the compactness (0.49) and a decrease in the water
340 content (0.14) of the agglomerates (Table 2). The dewatering generates slight mechanisms of
341 shrinking, which induce a decrease of the internal porosity and diameter of the agglomerates.
342 The drying stage contributes to the texturation of the grains by the densification of the
343 structure.

344 We observed that swelling and shrinking mechanisms generated by the successive steam
345 cooking and drying stages did not significantly affect the sphericity of the agglomerates
346 (Table 2). Water penetration and water extraction were in isotropic condition of the transfers
347 in this case. The sphericity ranged from 0.687 after the wet agglomeration stage and 0.662

348 after the drying stage. The wet agglomeration stage mainly determined the sphericity of the
349 agglomerates.

350 The microstructure of the dried agglomerates were observed by scanning electron microscopy
351 and compared to those of industrial couscous grains (Fig. 11). The dried agglomerates of
352 durum wheat semolina processed by the fluidised bed are characterized by irregular shape,
353 with very rough surfaces. The native semolina particles were clearly visible and
354 distinguishable in the dried agglomerates: they appeared as semi discrete particles glued to
355 each other. The dried agglomerates were not dense objects as internal porosity between
356 adjacent particles was observed demonstrating that solid fusion between the semolina
357 particles had not occurred. On the other hand, the classical couscous grains were
358 characterized by spherical shape with regular surfaces. The native semolina particles were
359 poorly visible in the grains, as they were partly glued to each other. The grains were almost
360 dense objects, as only little internal porosity can be observed demonstrating that solid fusion
361 between the semolina particles had largely occurred.

362 The mechanical properties of the agglomerates were measured by the mean force required to
363 compress them (Table 3). As expected, the wet agglomerates were characterized by lower
364 values of mechanical strength. The cooking and drying stage improved the mechanical
365 resistance of the agglomerates by increasing the mechanical strength (from 1.23 to 4.25 N).
366 However, the force required compressing the dried agglomerates produced by the fluidized
367 bed processing remained significantly lower than those measured for the classical couscous
368 grains (23 N).

369

370 4. Discussion

371 Granulation process by using the fluidized bed technology generates agglomerates of durum
372 wheat semolina with specific functional attributes. The present results describe the
373 potentialities of the fluidized bed to agglomerate wheat powders and investigate the process -
374 structure - properties relationships. The final properties of the dried agglomerates can be
375 discussed in regards with the classical couscous grains that are granulated by using low shear
376 mixers.

377

378

379 4.1 Hydrotextural analysis

380 Whatever the investigated process conditions using the standard semolina, the growth of the
381 wet agglomerates was characterized by one positive correlation between water contents and
382 diameters (Fig. 7a), and by a specific diameter ($d_{50} = 1600 \mu\text{m}$) that separated two
383 correlations between compactness and diameter: a negative slope at $d_{50} \leq 1600 \mu\text{m}$ and a
384 positive slope at $d_{50} \geq 1600 \mu\text{m}$ (Fig. 4b and 7b).

385 For the $d_{50} \leq 1600 \mu\text{m}$, a power law (Eq. 3) can be used to describe the relationship between
386 the compactness and the median diameter:

387

$$388 \phi = A_i d_i^{(D_f-3)} \quad (3)$$

389

390 where A_i is a prefactor characterizing the amplitude of the phenomenon and D_f is the mass
391 fractal dimension linked to the growth mechanism of the grain. The existence of a power law
392 relationship between the diameter and the compactness was demonstrated by Rondet et al.
393 (2010) during the wet agglomeration of various powders (kaolin, microcrystalline cellulose,
394 and calcium phosphate) using low shear mixers. Our results could be interpolated with a good
395 agreement by the power law (R^2 from 0.68 to 0.98) (Table 4). For $d_{50} \leq 1600 \mu\text{m}$, the
396 calculated values of the D_f factor (2.81 - 2.90) were not affected by the changes in the water
397 content. We only observed a decrease in the A_i values (from 0.48 to 0.32) when increasing
398 the water content. The prefactor is linked to the nuclei characteristics (compactness and
399 median diameter). Explanation of this variation needs to characterise the nuclei, elementary
400 association of semolina, which lead to the agglomerate structure by association, unrealised in
401 this study. By this analyse, mechanism for the wet agglomeration using the fluidized bed in
402 the cited process conditions can be considered as fractal morphogenesis for the smaller

403 structures ($d_{50} \leq 1600 \mu\text{m}$). Saad et al. (2011) also found a fractal-structuring model to
 404 describe the agglomeration of durum wheat semolina using a low shear mixer with a value of
 405 $D_f = 2.89$ and $A_i = 0.56$.

406 For $d_{50} \geq 1600 \mu\text{m}$, the value of the compactness slightly increased with the diameter of the
 407 agglomerates (Fig. 4b and 7b). This increase in compactness could be associated to the values
 408 of D_f close to 3. We could then suppose that some phenomena of densification of the grains
 409 occurred for the larger structures ($d_{50} \geq 1600 \mu\text{m}$) due to collisions with the wall and/or
 410 between the agglomerates themselves in the fluidized bed velocity field.

411 Considering the coarse semolina, the calculated value of $D_f = 2.56$ was lower than this
 412 obtained with the standard semolina (Fig. 9b). The lower value of D_f could indicate that the
 413 agglomeration process induces less mechanisms of densification on the investigated range of
 414 water contents.

415 The values of the physico-chemical characteristics of the wet agglomerates can also be
 416 discussed according to the hydrotextural analysis (Ruiz, Delalonde, Bataille, Baylac, &
 417 Dupuy de Crescenzo, 2005). The wet agglomerates were considered as the superposition of
 418 three dispersed phases: solid particles, liquid and gaseous phases. Three non-redundant
 419 variables provide a description of the system in term of mass and volume. The easiest chosen
 420 variables are generally the apparent volume (V), the mass of water (M_w) and the mass of solid
 421 (M_s). These variables were used to calculate the water content, the compactness and the
 422 saturation degree.

423 The hydrotextural diagram is limited in its upper part by the saturation curve, which
 424 represents the maximum water content that a grain of a given constant compactness can
 425 contain (Fig. 12). The saturation curve is calculated using Eq. (4):

426

$$427 \quad \phi_{sat} = \frac{1}{1+d_s^*w_{sat}} \quad (4)$$

428

429 Whatever the process conditions, the values of water content and compactness measured for
 430 the wet agglomerates were located under the saturation curve (Fig. 12). The wet agglomerates
 431 were porous structures at the scale of semolina particles (intraparticle porosity) and between
 432 particles (interparticle porosity). The range of variation of the compactness is essentially due
 433 to the particle re-arrangement. During the add of water, the filling of the interparticle voids did
 434 not occur by a simple remove of the air trapped. Capillary forces induced a re-arrangement

435 between the particles that was observed by a variation of the compactness (Fig. 12) and the
436 saturation degree.

437 The saturation degree increased (from 0.20 to 0.44) with an increase in the water content:
438 experimental values became closer to the saturation curve (Fig. 12). It was observed that the
439 growth could be fitted by a sigmoidal curve, comparable to this purposed by Ruiz et al.
440 (2005) :

441

$$442 \quad S(w) = 1 - \frac{1}{1 + e^{\frac{w-w_m}{d}}} \quad (5)$$

443

444 where w_m is the water content at $S=50\%$ and d is the reverse slope of the central quasi-linear
445 section of the sigmoidal curve. The relationship between water content and compactness (Fig.
446 12) means that inter granular arrangements led to an expansion followed by a densification of
447 the wet agglomerates. The first stage of expansion was induced with an addition of water: the
448 compactness decreased significantly and the saturation degree slightly increased. During the
449 second stage, the structures continued to grow up but with densification mechanisms due to
450 the capillarity influence. During this stage, the compactness slightly changed but the
451 saturation degree highly increased, which correspond to a high filling of the inter granular
452 voids. By associating Eq. (2) and Eq. (5), it was possible to describe the variation of the
453 compactness by the water content, the real densities of the solid and liquid phases and the two
454 parameters (w_m and d):

455

$$456 \quad \phi(w) = \frac{1}{1 + d_s^* w (1 - e^{-\frac{w-w_m}{d}})} \quad (6)$$

457

458 This relationship (Eq. 6) reduces to one (water content) the number of state variables
459 necessary and sufficient to describe the structure of the wet agglomerates of durum wheat
460 semolina produced by using the fluidized bed. In all case, our results could be interpolated
461 with a good agreement ($R^2 = 0.93$) by the relationship using Eq. (6), $w_m = 0.822$ and $d =$
462 0.513 . Our experimental results did not investigate the properties of the wet agglomerates
463 beyond this stage. Consolidation mechanisms could follow the stage of densification (Ruiz et
464 al. 2005). The values of water content and compactness of the agglomerates measured after
465 the agglomeration, cooking, and drying stages were presented on the hydro-textural diagram
466 (Fig. 13). The cooked and dried agglomerates were not dense grains as they remain under the

467 saturation curve. It can be observed that the phenomenon of retraction during the drying stage
468 increased the compactness of the grains. The dried grains of wheat semolina produced using
469 the fluidized bed technology were significantly different from the classical couscous grains,
470 which were more compact and almost saturated.

471

472

473 *4.2 Comparison with the couscous grains*

474 The dried grains of durum wheat semolina produced by the fluidized bed were more brittle
475 and less compact than the classical couscous grains. Using the fluidized bed technology, the
476 water addition stage was critical as it promotes the cohesion between the particles and the
477 physicochemical reactivity of the wheat components. The simultaneous agglomeration and
478 drying mechanisms restricted the contribution of the physicochemical reactivity of the wheat
479 components at the surface of particles, which were briefly in contact with water. Adhesion
480 between the particles could mainly come from physical forces, as capillary forces, and
481 liquid bridges involving superficial mechanisms. This may explain the lower compactness in
482 the grain prepared by fluidized bed processing. It can be supposed that partial starch
483 gelatinisation mechanisms only occur at the interface between the particles. The resulting
484 strength to compress the granules was significantly lower than those measured for the
485 classical couscous grains. The classical couscous grains were more compact and consolidated
486 by complete starch gelatinisation during the cooking stage. The fluidized bed technology
487 produced agglomerates of durum wheat semolina with specific functional attributes, which
488 were significantly different from those associated with the couscous grains.

489

490

491 *4.3 Process efficiency*

492 The process efficiency is related to the mass fraction of wet agglomerates with diameter
493 between 1000 and 2000 μm collected after the granulation stage. It is admitted that the wet
494 agglomeration stage controls for the process efficiency of the manufacture of the industrial
495 couscous grains (Abecassis et al., 2012). The classical low shear mixers generate low process
496 yield, with only 30 to 40% of grains with correct diameter and high amounts of out of
497 specification wet grains that do not have the correct diameter. In the present study, the
498 fluidized bed technology allowed reaching high values of yield of agglomeration, close to
499 66%. The fluidized bed granulation process generated low dispersion in the diameter of the
500 wet agglomerates, with a low proportion of the too large grains (only 10%), compared to

501 those obtained by a low shear mixer (20-25%). Fluidized bed technology could be a novel
502 way to produce high amounts of agglomerates of durum wheat semolina.

503 **5. Conclusion**

504 The agglomeration process using a fluidized bed has been found to produce agglomerates of
505 durum wheat with different attributes compared to those produced by granulation using low
506 shear mixers. The dried agglomerated grains obtained using the fluidized bed were less
507 compact than the traditional couscous grains manufactured using low shear mixers. Fluidized
508 bed granulation allowed producing higher amounts of agglomerates with diameter between
509 1000 and 2000 μm . Whatever the process conditions, the relationship between the
510 compactness and the median diameter can be described using a power law model. It allowed
511 demonstrating that agglomeration is driven by a fractal formation process for the wets
512 agglomerates with $d_{50} \leq 1600 \mu\text{m}$, and by densification mechanisms for the large
513 agglomerates ($d_{50} \geq 1600 \mu\text{m}$). This result indicates that the mechanisms which occur in the
514 fluidized bed present analogy between low shear mixer agglomeration. By using the
515 hydrotextural diagram, we proposed a specific model to describe the interparticle
516 arrangements, which associated expansion and densification of the wet agglomerates. The
517 relationship between the saturation degree and the compactness of the wet agglomerates was
518 reduced to only one state variables to describe the agglomeration mechanisms of durum
519 wheat semolina using a fluidized bed. This result is interesting because by using **Eq. (3) and**
520 **Eq. (6)**, we could predict the variation of the median diameter of agglomerates at different
521 water contents. Investigation of the nucleation phase needs to be conduct to describe the
522 agglomeration mechanism with more details. As in the case of agglomeration in high shear
523 mixer, nucleation regimes could be identified in relation to the hydrodynamic conditions of
524 the fluidized bed process.

525

526

527 **Acknowledgments**

528

529 The authors would like to thank the Agence Nationale de la Recherche (ANR ALID 2013)
530 for its financial support through the program “Dur Dur”.

531

532

533 **References**

- 534 AACC. (2000). *American Association of Cereal Chemists* (Official M). The Association, St.
535 Paul, MN, USA.
- 536 Abecassis, J., Cuq, B., Boggini, G., & Namoune, H. (2012). Other traditional durum derived
537 products. In *Durum wheat: chemistry and technology* (2nd Ed. AA, pp. 177–200).
- 538 AFNOR. (1970). Directives générales pour le dosage de l'azote avec minéralisation selon la
539 méthode de Kjeldahl. In *Norme Française V03-050*.
- 540 Banjac, M., Stakic, M., & Voronjec, D. (1998). Kinetics of agglomeration of milk powder in
541 a vibro-fluidized bed. In *11th International Drying Symposium* (pp. 998–1005).
- 542 Barkouti, A., Delalonde, M., Rondet, E., & Ruiz, T. (2014). Structuration of wheat powder by
543 wet agglomeration: Case of size association mechanism. *Powder Technology*, 252, 8–13.
- 544 Barkouti, A., Rondet, E., Delalonde, M., & Ruiz, T. (2012). Influence of physicochemical
545 binder properties on agglomeration of wheat powder in couscous grain. *Journal of Food*
546 *Engineering*, 111(2), 234–240.
- 547 Barkouti, A., Turchiuli, C., Carcel, J. A., & Dumoulin, E. (2013). Milk powder agglomerate
548 growth and properties in fluidized bed agglomeration. *Dairy Science and Technology*,
549 93, 523–535.
- 550 Bellocq, B., Ruiz, T., Delaplace, G., Duri, A., & Cuq, B. (2017). Screening efficiency and
551 rolling effects of a rotating screen drum used to process wet soft agglomerates. *Journal*
552 *of Food Engineering*, 195, 235–246.
- 553 Boerefijn, R., & Hounslow, M. J. (2005). Studies of fluid bed granulation in an industrial
554 R&D context. *Chemical Engineering Science*, 60(14), 3879–3890.
- 555 Cuq, B., Mandato, S., Jeantet, R., Saleh, K., & Ruiz, T. (2013). Agglomeration / granulation
556 in food powder production. In *Handbook of Food Powders: Processes and Properties*
557 (pp. 150–177). Woodhead publishing.
- 558 Dacanal, G. C., & Menegalli, F. C. (2010). Selection of operational parameters for the
559 production of instant soy protein isolate by pulsed fluid bed agglomeration. *Powder*
560 *Technology*, 203(3), 565–573.
- 561 Hafsa, I., Mandato, S., Ruiz, T., Schuck, P., Jeantet, R., Mejean, S., Chevallier, S., Cuq, B.
562 (2015). Impact of the agglomeration process on structure and functional properties of the
563 agglomerates based on the durum wheat semolina. *Journal of Food Engineering*, 145,
564 25–36.
- 565 Hébrard, A. (2002). *Granulation de semoules de blé dur*. Thèse de doctorat. Ecole nationale
566 supérieure d'agronomie de Montpellier.

- 567 Hemati, M., Cherif, R., Saleh, K., & Pont, V. (2003). Fluidized bed coating and granulation:
568 Influence of process-related variables and physicochemical properties on the growth
569 kinetics. *Powder Technology*, 130, 18–34.
- 570 Iveson, S. M., Litster, J. D., Hapgood, K. P., & Ennis, B. J. (2001). Nucleation, growth and
571 breakage phenomena in agitated wet granulation processes: a review. *Powder*
572 *Technology*, 117(1), 3–39.
- 573 Jacob, M. (2007). Granulation Equipment. In *Handbook of Powder Technology vol.11* (pp.
574 417–476). Amsterdam: Elsevier.
- 575 Ji, J., Fitzpatrick, J., Cronin, K., Fenelon, M. A., & Miao, S. (2017). The effects of fluidised
576 bed and high shear mixer granulation processes on water adsorption and flow properties
577 of milk protein isolate powder. *Journal of Food Engineering*, 192, 19–27.
- 578 Leuenberger, H., Puchkov, M., Krausbauer, E., & Betz, G. (2009). Manufacturing
579 pharmaceutical granules: Is the granulation end-point a myth? *Powder Technology*, 189,
580 141–148.
- 581 Morin, G., & Briens, L. (2014). A comparison of granules produced by high-shear and
582 fluidized-bed granulation methods. *Pharmaceutical Science and Technology*, 15(4),
583 1039–48.
- 584 Nienow, A. W. (1995). Fluidised Bed Granulation and Coating: Applications To Materials,
585 Agriculture and Biotechnology. *Chemical Engineering Communications*, 139(1), 233–
586 253.
- 587 Oulahna, D., Hebrard, A., Cuq, B., Abecassis, J., & Fages, J. (2012). Agglomeration of
588 durum wheat semolina: Thermodynamic approaches for hydration properties
589 measurements. *Journal of Food Engineering*, 109(3), 619–626.
- 590 Palzer, S. (2011). Agglomeration of pharmaceutical, detergent, chemical and food powders -
591 Similarities and differences of materials and processes. *Powder Technology*, 206, 2–17.
- 592 Pathare, P. B., Baş, N., Fitzpatrick, J. J., Cronin, K., & Byrne, E. P. (2012). Production of
593 granola breakfast cereal by fluidised bed granulation. *Food and Bioproducts Processing*,
594 90(3), 549–554.
- 595 Philippsen, C. G., Vilela, A. C. F., & Zen, L. D. (2015). Fluidized bed modeling applied to
596 the analysis of processes: Review and state of the art. *Journal of Materials Research and*
597 *Technology*, 4(2), 208–216.
- 598 Rambali, B., Baert, L., & Massart, D. L. (2001). Using experimental design to optimize the
599 process parameters in fluidized bed granulation on a semi-full scale. *International*
600 *Journal of Pharmaceutics*, 220, 149–160.

- 601 Rieck, C., Hoffmann, T., Bück, A., Peglow, M., & Tsotsas, E. (2015). Influence of drying
602 conditions on layer porosity in fluidized bed spray granulation. *Powder Technology*,
603 272, 120–131.
- 604 Rondet, E., Delalonde, M., Ruiz, T., & Desfours, J. P. (2010). Fractal formation description
605 of agglomeration in low shear mixer. *Chemical Engineering Journal*, 164(2–3), 376–
606 382.
- 607 Ruiz, T. (2012). *Explorations d'archétypes de mélanges grains , gouttes , bulles*. Habilitation
608 à diriger des recherches. Université de Montpellier 2.
- 609 Ruiz, T., Delalonde, M., Bataille, B., Baylac, G., & De Crescenzo, C. D. (2005). Texturing
610 unsaturated granular media submitted to compaction and kneading processes. *Powder*
611 *Technology*, 154(1), 43–53.
- 612 Ruiz, T., Rondet, E., Delalonde, M., & Desfours, J. P. (2011). Hydro-textural and consistency
613 surface states of humid granular media. *Powder Technology*, 208(2), 409–416.
- 614 Saad, M. M., Barkouti, A., Rondet, E., Ruiz, T., & Cuq, B. (2011). Study of agglomeration
615 mechanisms of food powders: Application to durum wheat semolina. *Powder*
616 *Technology*, 208(2), 399–408.
- 617 Saleh, K., & Guigon, P. (2009). Mise en œuvre des poudres Granulation humide : bases et
618 théorie. *Techniques de L'ingénieur*, J2254.
- 619 Smith, P. G., & Nienow, A. W. (1983). Particle growth mechanisms in fluidised bed
620 granulation - the effect of process variables. *Chemical Engineering Science*, 38(8).
- 621 Turchiuli, C., Eloualia, Z., El Mansouri, N., & Dumoulin, E. (2005). Fluidised bed
622 agglomeration: Agglomerates shape and end-use properties. *Powder Technology*, 157,
623 168–175.
- 624 Turchiuli, C., Fuchs, M., Bohin, M., Cuvelier, M. E., Ordonnaud, C., Peyrat-Maillard, M. N.,
625 & Dumoulin, E. (2005). Oil encapsulation by spray drying and fluidised bed
626 agglomeration. *Innovative Food Science and Emerging Technologies*, 6, 29–35.
- 627 Turchiuli, C., Smail, R., & Dumoulin, E. (2013). Fluidized bed agglomeration of skim milk
628 powder: Analysis of sampling for the follow-up of agglomerate growth. *Powder*
629 *Technology*, 238, 161–168.
- 630 Zhai, H., Li, S., Andrews, G., Jones, D., Bell, S., & Walker, G. (2009). Nucleation and
631 growth in fluidised hot melt granulation. *Powder Technology*, 189(2), 230–237.
- 632
- 633

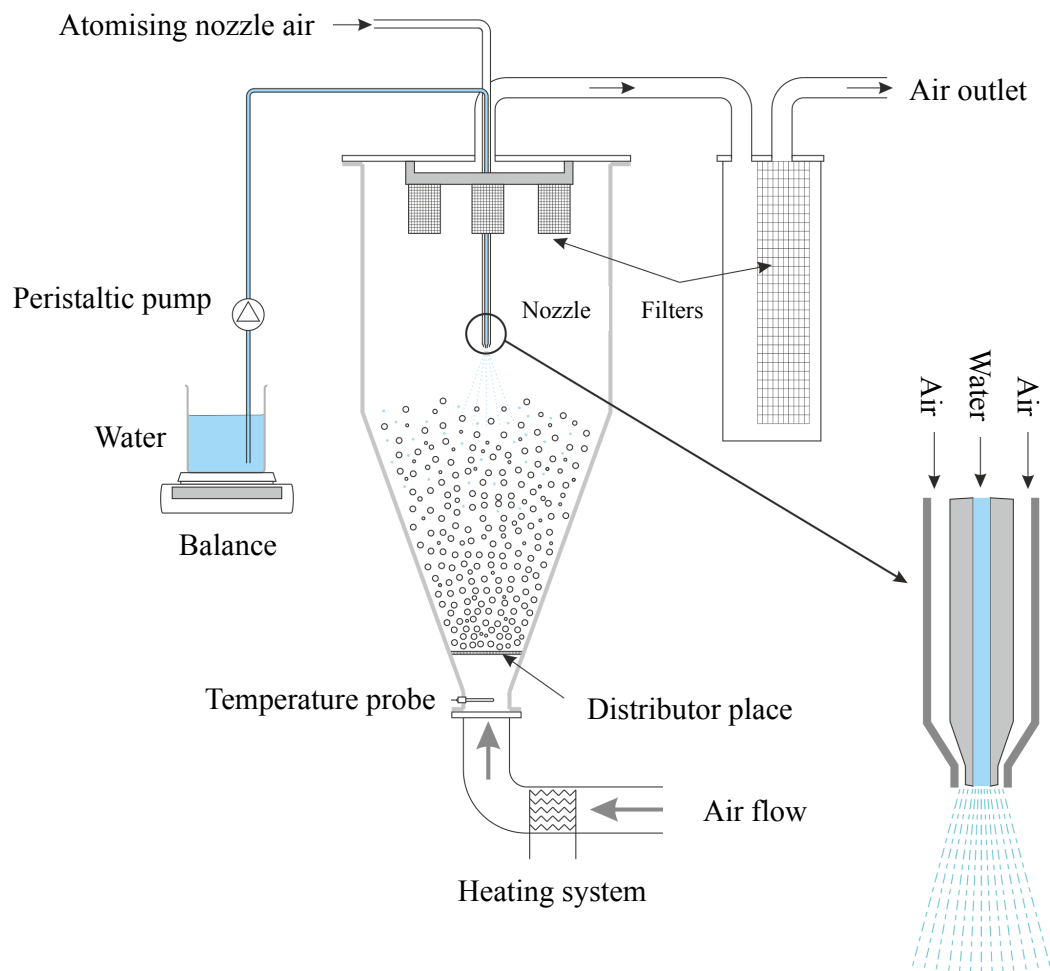
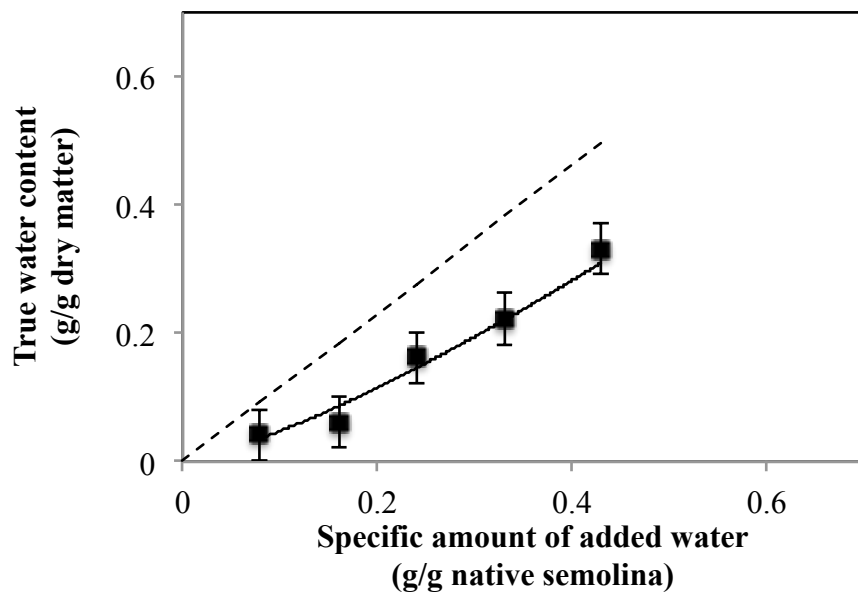


Fig. 1. Schematic description of the fluidized bed equipment.

634

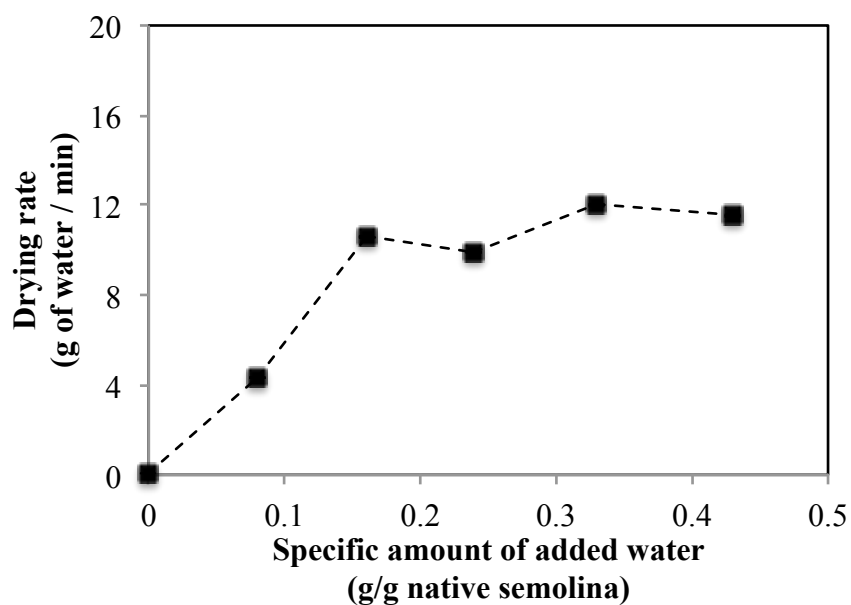
635

636



637

(a)



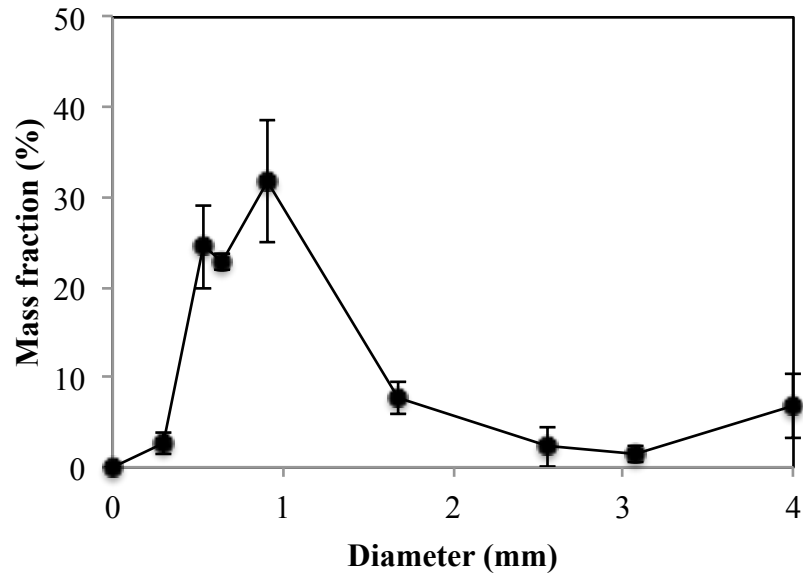
638

(b)

639

640 **Fig. 2.** Experimental curves of the true water contents (a) and the drying rates (b) as a
 641 function of the specific amount of added water in the fluidized bed (the dotted line in figure
 642 (a) corresponds to the apparent process water content).

643

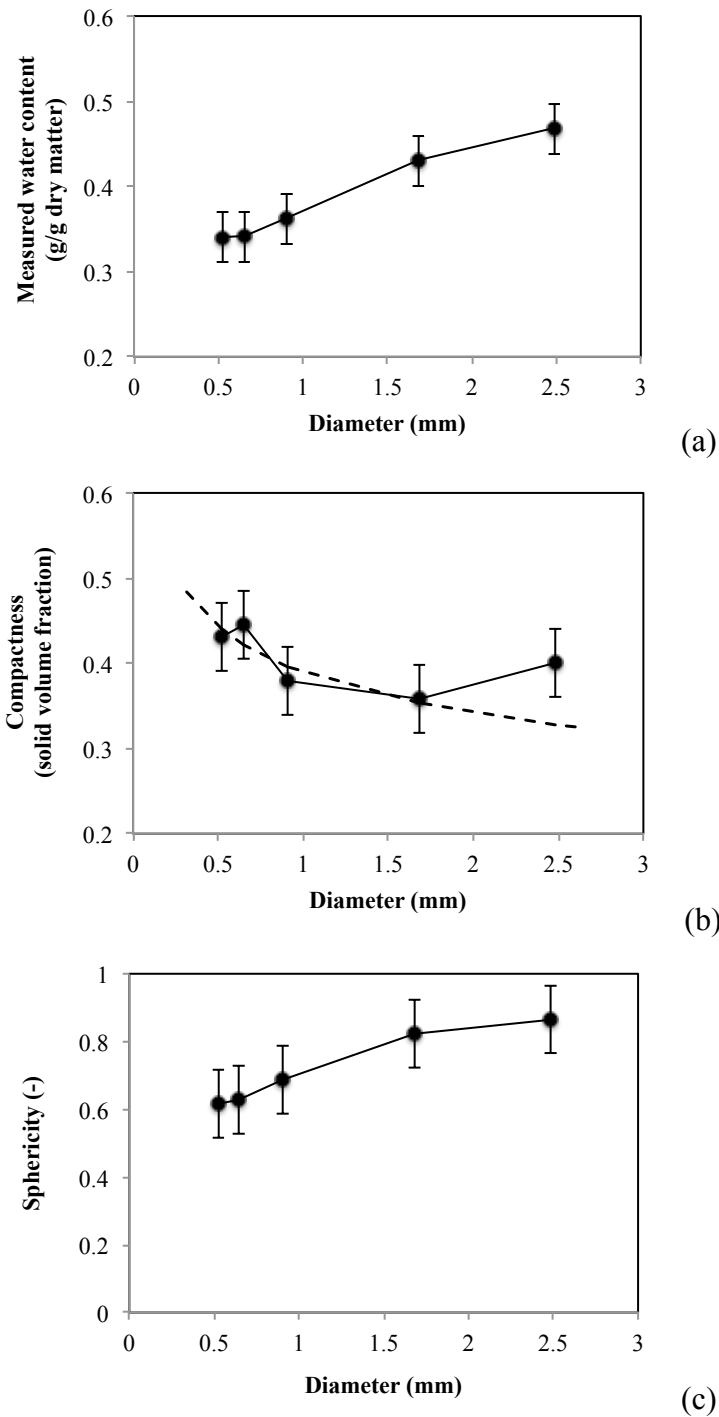


644

645

646 **Fig. 3.** Distribution curve of the diameters of the wet agglomerates processed by the fluidized
 647 bed (experiments using standard semolina and true water content of 0.37 g/g dry matter).

648



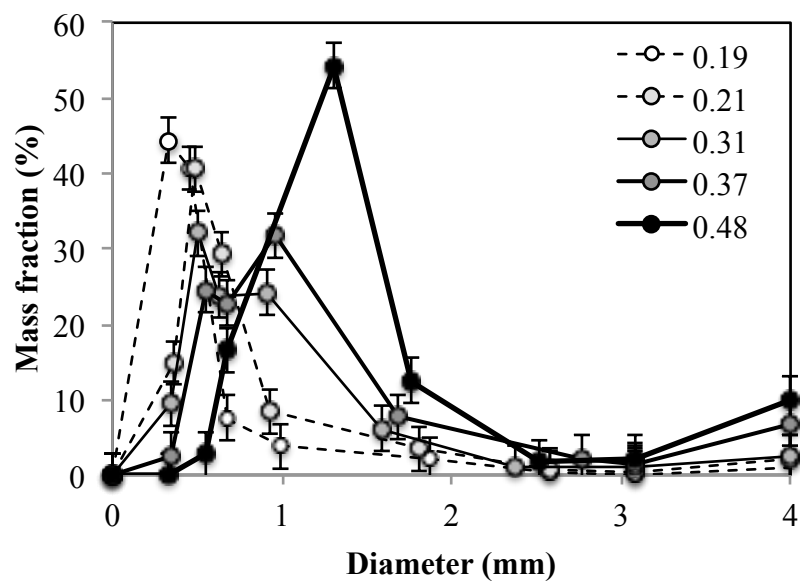
649

650

651

652 **Fig. 4.** Distribution curves of the measured values of water content (a), compactness (b) and
 653 sphericity (c), as a function of the diameter of the wet agglomerates processed by the
 654 fluidized bed (experiments using standard semolina and true water content of 0.37 g/g dry
 655 matter). (The dotted line in figure (b) is the fractal model using Eq. (3))

656



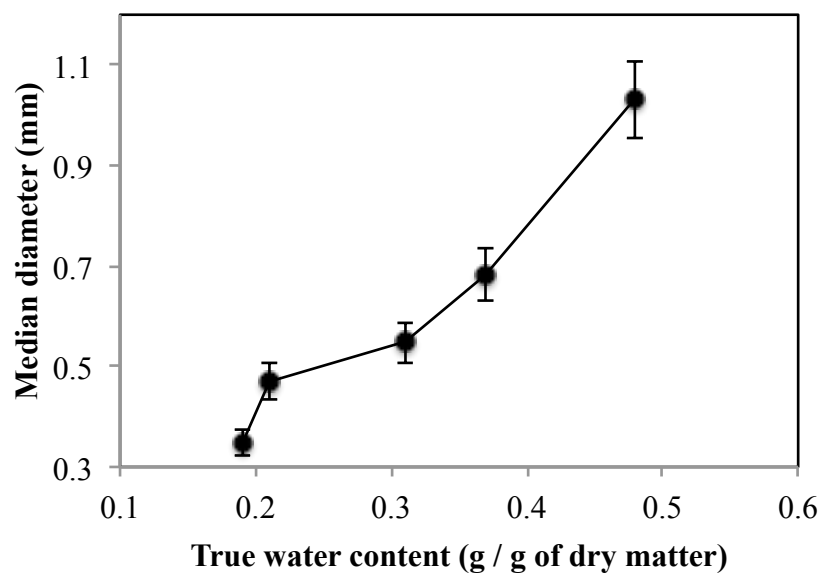
657

658

Fig. 5. Impact of the true water content on the distribution curves of the diameters of wet agglomerates processed by the fluidized bed (experiments using standard semolina).

659

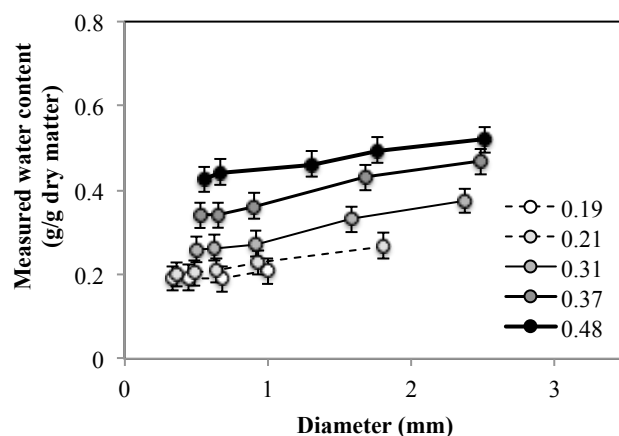
660



661

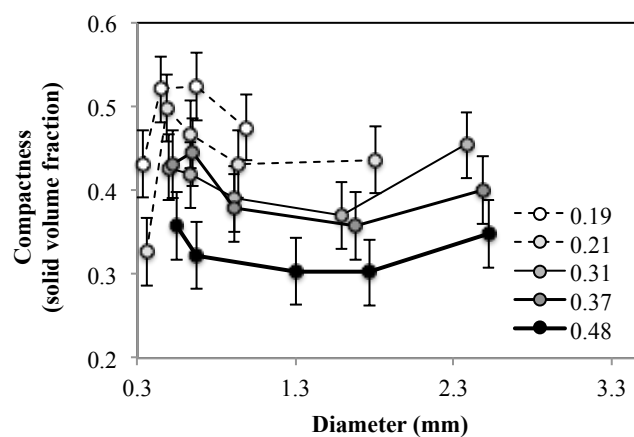
662 **Fig. 6.** Impact of the true water content on the median diameters (d_{50}) of wet agglomerates
 663 processed by the fluidized bed.

664



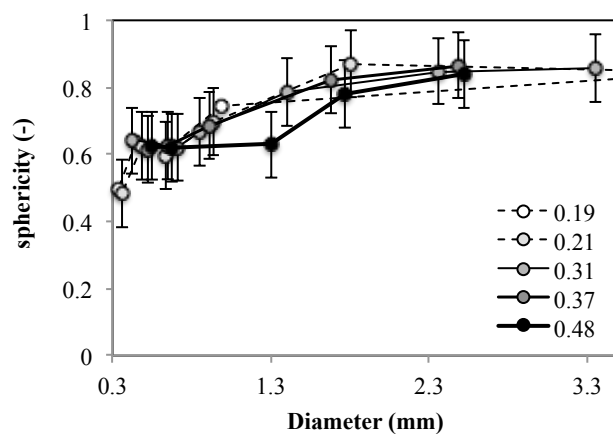
665

(a)



666

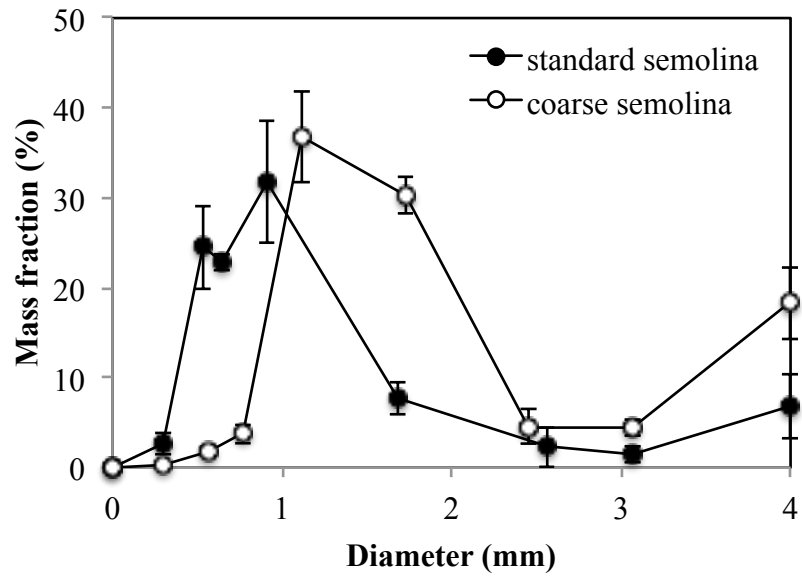
(b)



667

(c)

668 **Fig. 7.** Distribution curves of the measured values of the water content (a), compactness (b),
 669 and sphericity (c), as a function of the diameter of wet agglomerates processed by the
 670 fluidized bed at different true water contents (from 0.19 to 0.48 g / g of dry matter).
 671



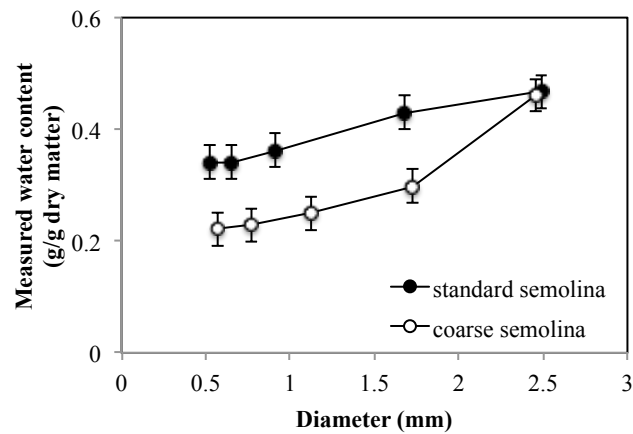
672

673

Fig. 8. Impact of the diameter of the semolina on the distribution curves of the diameters of wet agglomerates processed by the fluidized bed.

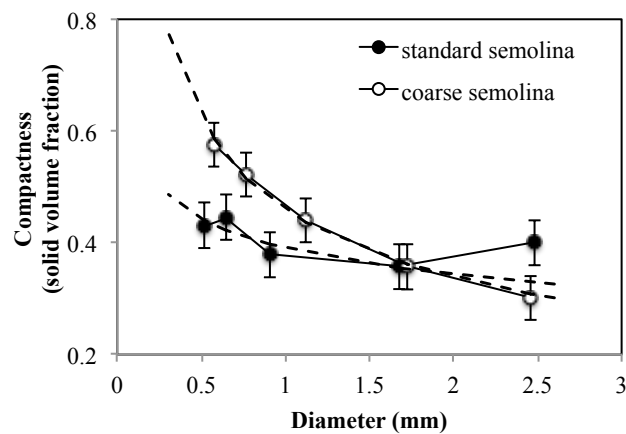
674

675



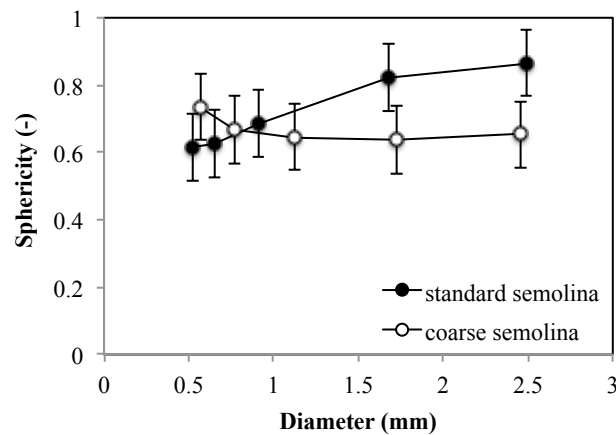
676

(a)



677

(b)

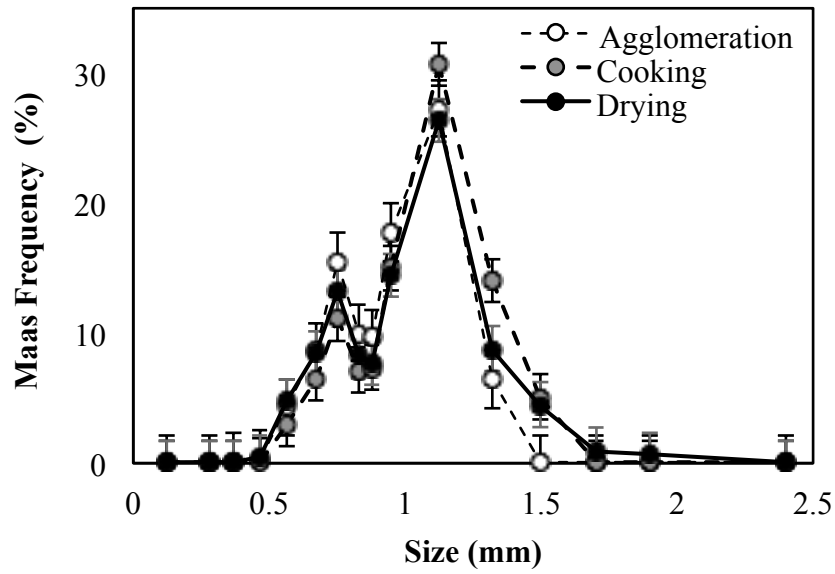


678

(c)

679 **Fig. 9.** Impact of the diameter of the particles of semolina on the values of water content (a),
 680 compactness (b), and sphericity (c) as a function of the diameter of wet agglomerates
 681 processed by the fluidized bed. (The dotted lines figure (b) is the power law model using Eq.
 682 (3)).

683



684

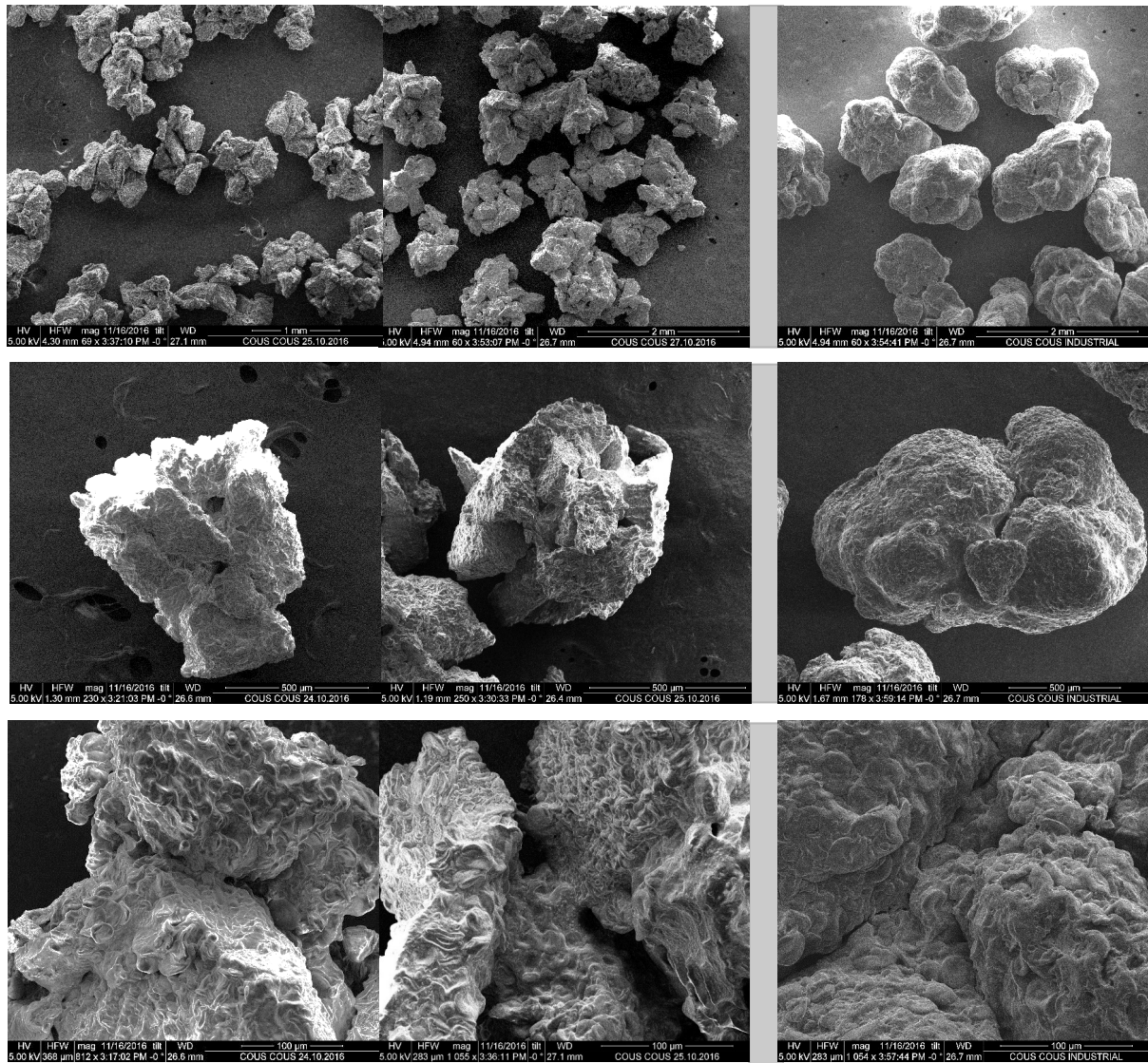
685

686

687

688

Fig. 10. Distribution curves of the diameters of the agglomerates after the agglomeration, cooking and drying stages (experiments using standard semolina and true water content of 0.37 g/g dry matter).



(a)

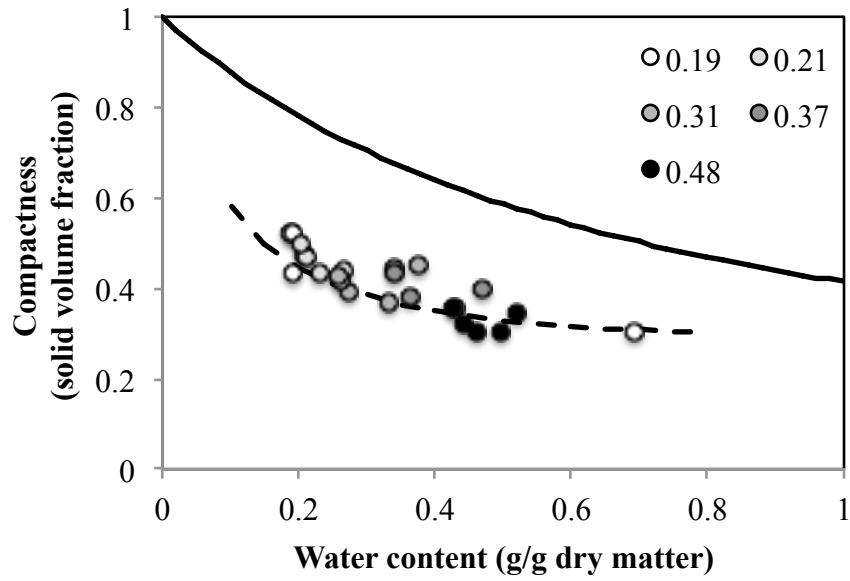
(b)

689

690 **Fig. 11.** Microstructure of the agglomerates based on of durum wheat semolina prepared with
 691 the fluidized bed (a) and commercial couscous grains (b) at different magnifications.

692

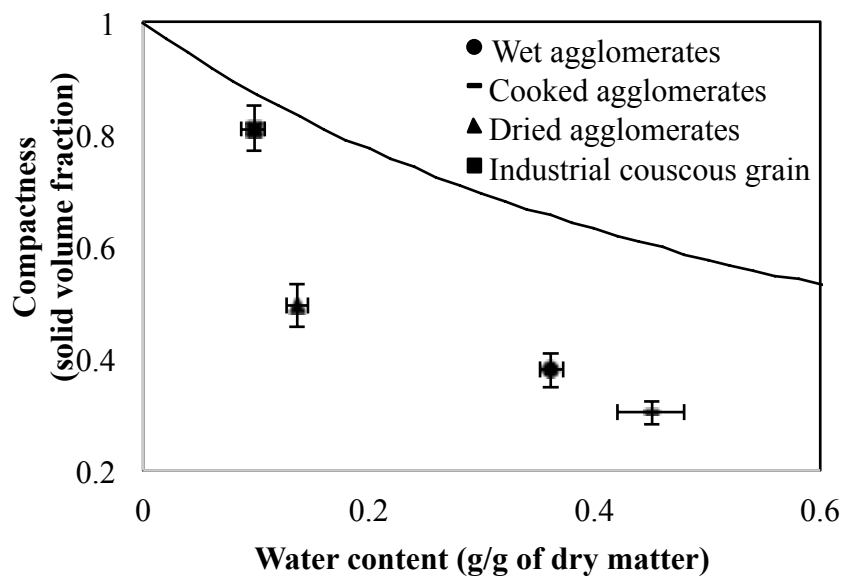
693



694

695 **Fig. 12.** Hydrotextural description (compactness vs. water content) of the wet agglomerates
 696 of durum wheat semolina according to the true water content. The black line represents the
 697 saturation curve. The dotted line represents the model curve (Eq. 6)

698



699

700 **Fig. 13.** Hydro-textural description (compactness vs. water content) of the agglomerates of
 701 durum wheat semolina after the agglomeration, cooking, or drying stage. Comparison with an
 702 industrial couscous grains.

703

704 **Table 1**

705 Physicochemical characteristics of the two-selected durum wheat semolina.

706

	Standard semolina	Coarse semolina
Water content (g/g dry semolina)	14.8 (± 0.5)	15.0 (± 0.5)
Protein content (g/g dry matter)	12.4 (± 0.1)	11.6 (± 0.1)
Particle diameter - d_{10} (μm)	66 (± 1)	434 (± 1)
Particle diameter - d_{50} (μm)	283 (± 1)	619 (± 1)
Particle diameter - d_{90} (μm)	542 (± 4)	888 (± 1)
True density	1.415 (± 0.005)	1.453 (± 0.003)
Apparent density	1.372 (± 0.007)	1.414 (± 0.006)
Compactness	0.845 (± 0.009)	0.846 (± 0.009)

707

708

709 **Table 2**

710 Physicochemical characteristics of the agglomerates after the cooking stage and after the
 711 drying stage.

712

	d ₅₀ (mm)	Span (-)	Water content (g / g dry matter)	Compactness (-)	Sphericity (-)
Wet	0.91 (± 0.05) ^a	0.47 (± 0.02) ^a	0.36 (± 0.02) ^c	0.38 (± 0.02) ^b	0.687 (± 0.02) ^c
Cooked	1.00 (± 0.01) ^b	0.53 (± 0.02) ^b	0.45 (± 0.06) ^d	0.30 (± 0.03) ^a	0.572 (± 0.05) ^a
Dried	0.95 (± 0.02) ^a	0.64 (± 0.02) ^c	0.14 (± 0.01) ^b	0.49 (± 0.04) ^c	0.662 (± 0.01) ^b
Industrial	1.60 (± 0.01) ^c	0.56 (± 0.1) ^b	0.10 (± 0.01) ^a	0.81 (± 0.04) ^d	0.844 (± 0.01) ^d

713

714 Values are means (\pm standard deviation).

715 Values in column with the same letter were not significantly different (P<0.05).

716

717

718 **Table 3**

719 Comparison of the mechanical strength of the wet agglomerates and of the dried
 720 agglomerates of durum wheat semolina prepared with the fluidized bed. Comparison with
 721 commercial couscous grains.

	Strength (N)
Wet agglomerates	1.23 (± 0.89) ^a
Dried agglomerates	4.25 (± 1.19) ^b
Classical couscous grains	22.99 (± 5.60) ^c

722 Values are means (\pm standard deviation).

723 Values in column with the same letter were not significantly different (P<0.05).

724

725 **Table 4**

726 Model parameters, coefficients of correlation and absolute deviations for all the experiments,
727 using the power law Eq. (3).

Semolina	w	A_i	D_f	R^2	Absolute deviation
Standard	0.19	0.48	2.87	0.69	0.25
	0.21	0.45	2.90	0.68	0.12
	0.31	0.39	2.87	0.98	0.12
	0.37	0.39	2.81	0.83	0.13
	0.48	0.32	2.87	0.81	0.10
Coarse	0.30	0.46	2.56	0.99	0.03

728